

Fluid and kinetic description of plasmas

This is a corrected and slightly updated version of a document first proposed during a training held on-line during the week 17th May to 21st May 2021 in the frame of the trainings proposed by the Doctoral School “Astronomie et Astrophysique d’Ile de France”. The training does not require any previous knowledge in the field of plasma physics or numerical computation. Notions and tools necessary to run and analyze the simulations, mainly through images, plots and movies, will be introduced gradually. The proposed questions are merely meant to guide reflection. Feel free to run your own simulations if you find the proposed ones excessively boring.

1 Introduction

This document provides the instructions to simulate a plasma using two different codes: a fluid code (*MHD*¹ code) and a collisionless code (*hybrid*² code).

In section 2 of this document you’ll find a short overview on how to run both the *MHD* code and the *hybrid* code and how to load the results in the visualization software ParaView.³

In Sections 3 to 6, you’ll find instructions on how to run various simulations along with some examples of data visualization with ParaView. Towards the end of each section there is a short list of relatively generic questions which may help you to analyze the simulations.

You do not need to understand how the codes work, there is no time for this. Rather use the codes as “black boxes”. The idea here is that you run the proposed problems and try to unveil the underlying physical mechanisms by analyzing plots, images and movies.

2 Quick start

Here you will learn how to run a simulation and how to load the data produced by the simulation into the visualization software ParaView. We assume that the *MHD* code and the *hybrid* code are already installed on your Linux (or possibly macOS).

1. MHD stands for magnetohydrodynamics. In principle, MHD codes should be used to simulate plasmas with characteristic spatial scales much larger than the collisional mean free path of the particles it contains (ions and electrons).

2. In a hybrid code, ions are treated as charged point particles moving in a self-consistent electromagnetic field defined on a discrete grid. Electrons are treated as a massless, charge neutralizing, fluid. Hybrid codes are used to simulate plasmas where the characteristic spatial scales are much smaller than the collisional mean free path of the ions.

3. It is assumed that the two codes and the software ParaView are already installed and working on your PC or VM (Virtual Machine).

The files generated by the simulations are [csv](#) files. They can be loaded directly into ParaView (from within the ParaView window: File → Open). However, for the non experienced user it may be more instructive to load the files into ParaView using a pre-existing treatment pipeline called *state files* (files with extension [.pvsm](#)). The treatment applied to the loaded data appears explicitly in the Pipeline Browser pane which is generally located on the left in the ParaView window.

2.1 Run a MHD simulation and import data in ParaView

- Open a terminal and browse to the top folder of the installed MHD code (the folder with the file [main000.f](#))
- In the terminal type: [./run_CIAS/run_test.sh](#)
- If code compiling and execution terminate successfully, the message **STOP fin** appears in the terminal followed by the path to the folder where the results have been stored (a sub-folder of the **DATA** folder including date and time information).
- Start ParaView. For example from within the terminal by typing [paraview &](#)
- In the upper toolbar in the ParaView window select: File → Load State → browse to the folder **PVSM_CIAS** → select file [read_MHD.pvsm](#) → select option **Choose File Names** → Click on the tab **[. . .]** → Browse to the folder where the simulation results have been stored and select the Group of files [Test_xy_all_..csv](#) → OK → OK

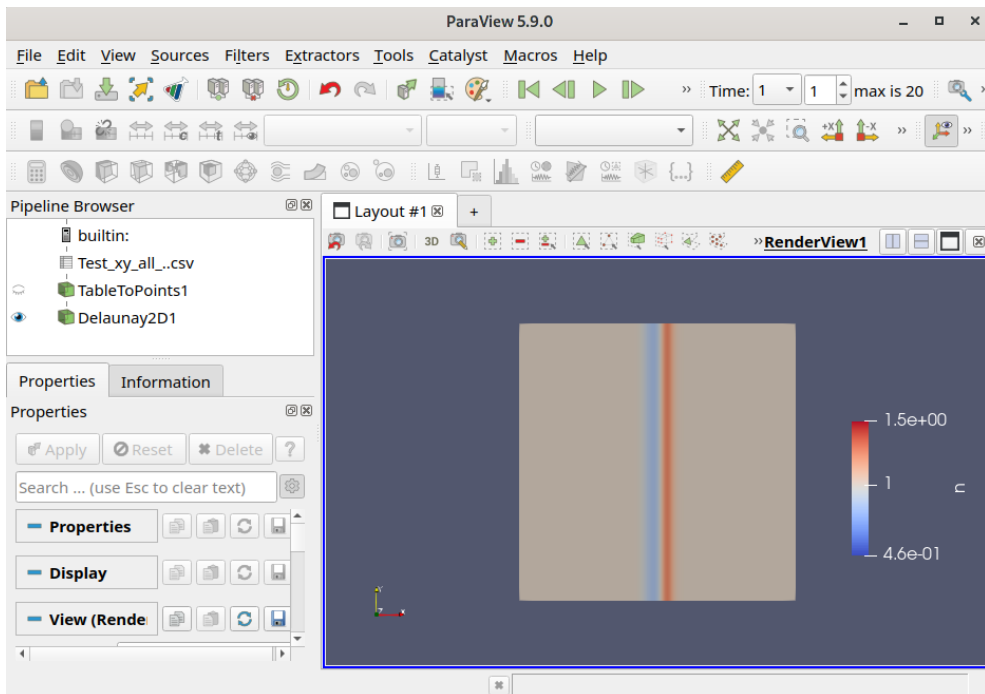


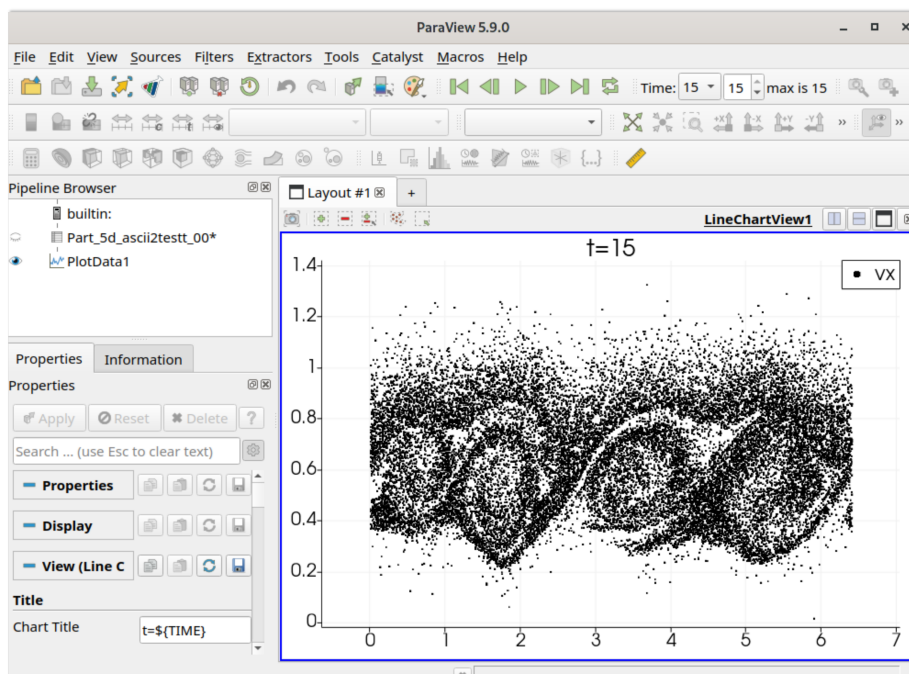
Figure 1. ParaView window after successful import of data from test simulation (file [./run_CIAS/run_test.sh](#))

2.2 Run a hybrid simulation and import data in ParaView

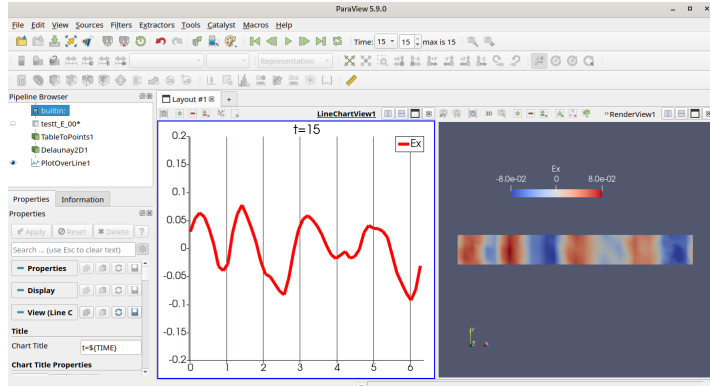
- Open a terminal and browse to the main folder of the installed hybrid code and proceed to the sub-folder `input` (the folder containing the file `run`)
- In the terminal window type: `./run ./run_CIAS/test.in`
- If code compiling and execution terminate successfully, the message `Results in folder:` appears in the terminal followed by the full path to the folder where the data has been stored.

NB: The hybrid code produces 3 different groups of files which need to be loaded separately into ParaView. These are **(1)** the files with the position and velocities of the particles, **(2)** the files with the electric field and **(3)** the files with the magnetic field and various moments of the ions such as their number density, their mean velocity or their thermal pressure.

- To load the file with the position and velocity of particles into ParaView:
 - Start ParaView. For example from within the terminal by typing `paraview &`
 - File → Load State → browse to the folder `Plot/Paraview` → select file `read_particles.pvsm` → select option `Choose File Names` → Click on the tab `[...]` → browse to the folder where the simulation results have been stored and select the Group `Part_5d_ascii2testt...csv` → OK → OK



- To load the file with the electric field into ParaView:
 - Start ParaView (if necessary).
 - File → Load State → browse to the folder `Plot/Paraview` → select file `read_electric.pvsm` → select option `Choose File Names` → Click on the tab `[...]` → browse to the folder where the simulation results have been stored and select the Group `testt_E...csv` → OK → OK



- To load the file with the magnetic field and moments of particles into ParaView:
 - Start ParaView (if necessary)
 - File → Load State → browse to the folder [Plot/Paraview](#) → select file `read_mag_field_and_moments.pvsm` → select option [Choose File Names](#) → Click on the tab `[...]` → browse to the folder where the simulation results have been stored and select the Group [testt_A...csv](#) → OK → OK

More complex ParaView state file (extension .pvsm) are presented in the next sections. They should suffice to generate the plots required to interpret the simulation. Also note that various tutorials can be found on the web, e.g. <https://www.paraview.org/tutorials>.

3 Weak perturbations (PT1)

In this first numerical experiment we consider the propagation of a small perturbation in a compressible fluid (section 3.1) and in a collisionless plasma (section 3.2). The perturbation is initiated by a thin slab of fluid slowly moving with respect to the surrounding resting fluid. The slab is translationally invariant in the y direction and moving in the x direction. We qualify the perturbation as “small” if the initial velocity of the slab is small with respect to the sound speed $c=\sqrt{\gamma T}$, where γ is the adiabatic index and T the fluid temperature⁴.

3.1 Fluid case: simulation B1 (run_B1.sh)

Use the MHD code. Open a terminal and change to the main folder of the code (e.g. where the file makefile is located). Start the simulation by typing `./run_CIAS/run_B1.sh` Under successful compilation and execution, the full path to the folder where the results are stored appears as a message in the terminal.

Change to the folder where the results are stored (e.g. the file `B1_xy_all_0000.csv`) and start ParaView with the command [paraview &](#)

⁴. In the MHD code, unless specified otherwise, we use the normalization $k_B/m = \mu_0 = 1$, where k_B is the Boltzmann constant, μ_0 the permeability of vacuum and m the average mass of the plasma particles. Thus, in a fully ionized, overall neutral, electron proton plasma $m \approx m_p/2$ and the Alfvén speed is $v_A^2 = B^2/(nm)$, where $n = n_e + n_p$ is the total plasma density (electron + proton).

Once in ParaView select the tab **File** —> **Load State** and select the state **B1.pvsm** in the sub folder **PVSM_CIAS** of the main code folder. In the Load State Options window select the option **Choose File Names** and load all files generated by the simulation by right-clicking on the Group **B1_xy_all_.csv** After loading the group of files the following image should appear in the ParaView window:

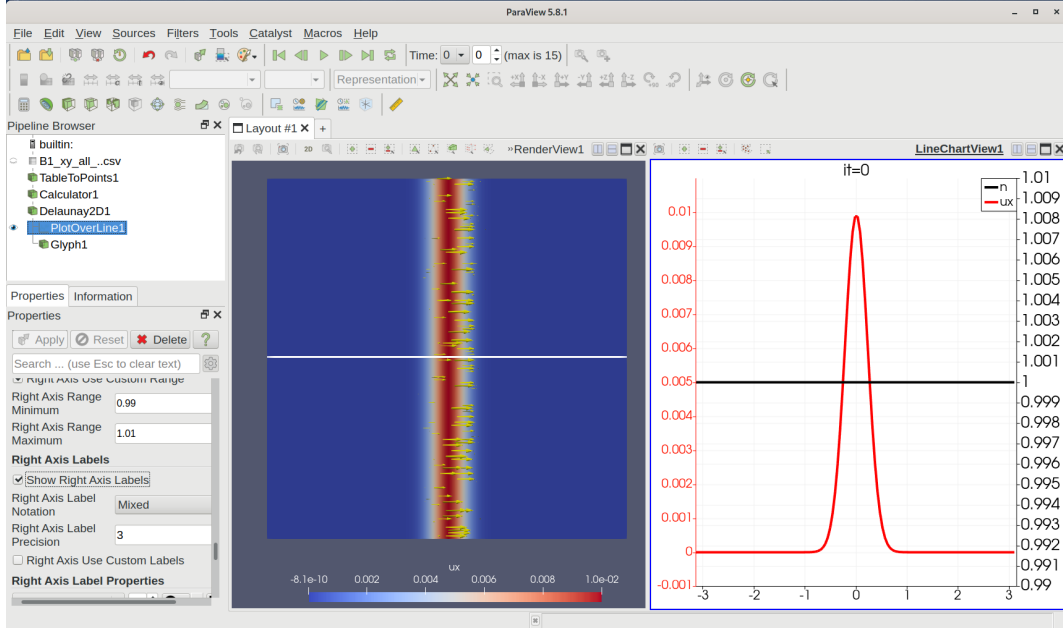


Figure 2. Initial condition for simulation B1. System is uniform except for a positive velocity bump centered on $x=0$. The system is invariant in the y direction. The figure has been produced using the ParaView state file **B1.pvsm**

Theory: The one-dimensional fluid equations, neglecting viscosity and conductivity are given by the continuity, momentum and energy equations (γ is the polytropic index, $\partial_x \equiv \partial / \partial x$, $\partial_t \equiv \partial / \partial t$)

$$\partial_t \varrho = -\partial_x(u\varrho) \quad (\text{continuity}) \quad (1)$$

$$\partial_t u = -u\partial_x u - (1/n)\partial_x p \quad (\text{momentum}) \quad (2)$$

$$\partial_t p = -u\partial_x p - \gamma p\partial_x u \quad (\text{adiabatic one-fluid closure}) \quad (3)$$

Two modes propagating in opposite directions exist which do satisfy $\partial_t u \pm c\partial_x u = 0$ where $c = \sqrt{\gamma p_0 / \varrho_0} = \sqrt{\gamma T_0}$ is the sound speed, with p_0 and ϱ_0 the average pressure and mass density. The velocity, density and pressure fluctuations associated with the two modes are related through $u/c = \pm \delta\varrho/\varrho_0$ and $\delta p/p_0 = \gamma \delta\varrho/\varrho_0$ where $\delta\varrho \equiv \varrho - \varrho_0$ and $\delta p \equiv p - p_0$. Note that in the code the normalized temperature is defined as $T = p/n$.

3.2 Hybrid case: simulations RG1, RG4, RG3, RG5

Use the hybrid code: Open a terminal and change to the sub-folder named **input**. In order to run simulation RG1 type **./run ./run_CIAS/RG1.in** which will run the

hybrid code using the configuration file [RG1.in](#) located in the sub-folder [run_CIAs](#). Files produced by the simulation are stored in the sub-folder [DATA](#).

There are 4 runs available. The runs only differ by the electron temperature through the definition of a different electron beta (defined as `[betae]` in the configuration files) which, in normalized units⁵ is given by $\beta_e \equiv 2n_e T_e / B_0^2$, representing the ratio of the pressure of the electrons $p_e = n_e T_e$ and the magnetic pressure $p_B = B^2/2$. Note that the magnetic field $B_0=1$ is directed along the x axis so that it has no effect on the ions' dynamics in that direction. Also, the average electron density in the system is $n_e=1$ so that the normalized electron temperature in the simulations is just $T_e=0.5\beta_e$

Run	RG1	RG4	RG3	RG5
β_e	0.05	0.25	0.5	2.5

In all simulations the ion temperature in the x direction (parallel to B_0) is $T_{i\parallel} = 0.5\beta_{i\parallel} = 0.125$.

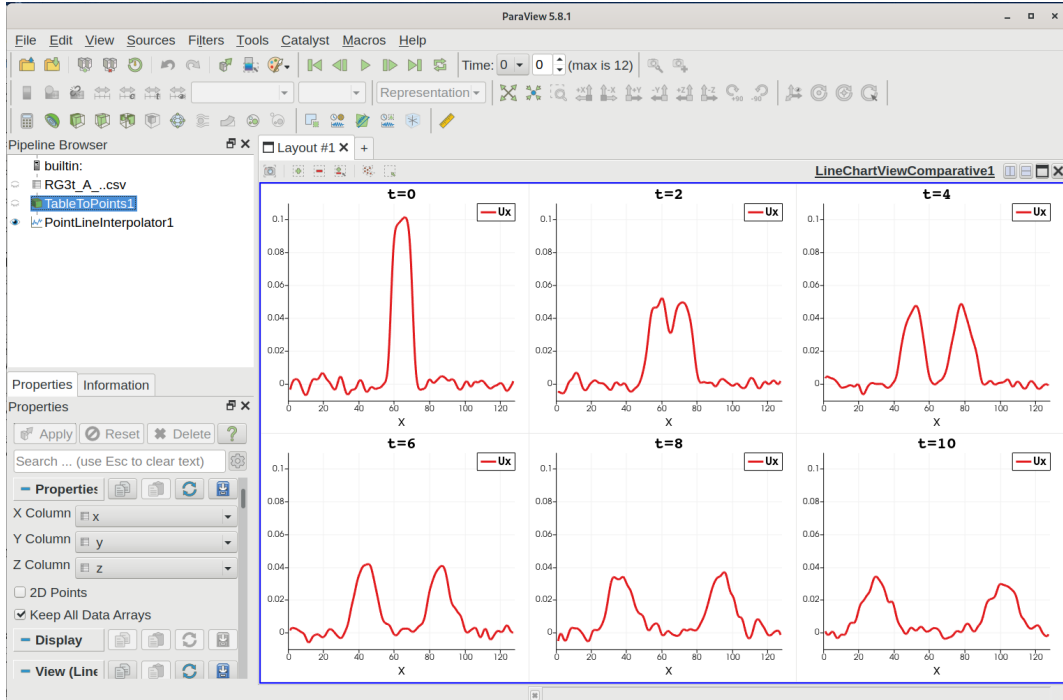


Figure 3. Evolution of the x component of the “fluid velocity” of the ions in simulation RG3. Figure has been obtained using the ParaView state file [RG3_6.pvsm](#).

In fact, even in the collisionless situation where the particles are essentially free streaming (namely the case RG1) the behavior of the system is very similar to the

5. In the hybrid code normalizations do slightly differ from the normalizations in the MHD code . In the hybrid code the Boltzmann constant, the permeability of vacuum and the proton mass are: $k_B = \mu_0 = m_p = 1$. Electrons are massless, i.e. $m_e = 0$ so that the normalized Alfvén speed is $v_A^2 = B^2/n$ where $n = n_e = n_p$.

fluid (collisional) case, showing a density “hole” moving to the left and a density “bump” moving to the right, both associated with a positive velocity bump. A picture of the evolution of the particles in (x, v_x) phase space for the case RG1 is shown in the next figure

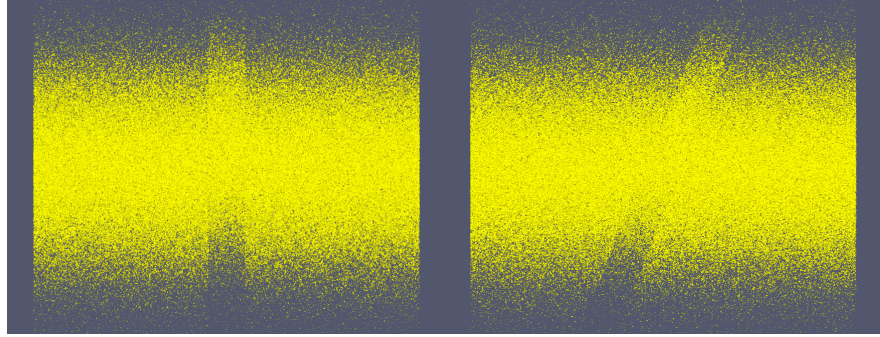


Figure 4. Particles from simulation RG1 in the v_x versus x phase space at $t = 0$ (left) and at $t > 0$ (right). Note how particles associated with the initial velocity bump evolve in time. The state file [RG1_particles_vx_x.pvsm](#) has been used to produce the plots.

Theory: The velocity of an ion (charge q , mass m) in the x direction, i.e. along the magnetic field, changes under the effect of an electric field component E_x

$$\frac{dv_x}{dt} = E_x(x, t) q/m \quad (q = e = m = 1 \text{ in code units}). \quad (4)$$

In the hybrid approximation where $n = n_i \approx n_e$ (therefore assuming singly charged ions) and the mass of electron is zero, the electrostatic field E can be written as (a reduced version of Ohm’s law):

$$eE_x = -(1/n_e) \partial p_e / \partial x \quad (5)$$

where $p_e = n_e T_e \propto n_e^\gamma$. The first two fluid equations describing the ions’ motion can therefore be written as :

$$\partial_t n = -\partial_x(un) \quad (6)$$

$$\partial_t u = -u \partial_x u - (1/n) \partial_x p, \text{ where } p = p_e + p_i \quad (7)$$

where the pressure p is intended to represent the p_{xx} component of the pressure tensor. A simple energy equation similar to (3) is not easily written in this case as electrons and protons may behave very differently. The modes phase velocity may therefore depend on various parameters including the mode’s wavelength. In the

limit $p_i \ll p_e$ ⁶ a propagating mode exists which is reminiscent of the standard sound mode with a phase velocity $v_\phi = \sqrt{\gamma_e T_e + \gamma_i T_i}$, where $\gamma_e = 5/3$, a value often adopted in hybrid codes and $\gamma_i = 3$ ⁷. Given the above fluid equations, the relations for the eigenmodes are those of the standard sound mode: $\pm \delta u / v_\phi = \delta n / n = (1/\gamma) \delta p / p$.

Sample questions:

- How can a positive velocity bump move with a negative phase velocity (i.e. to the left)?
- Measure the propagation velocity of the perturbations in the fluid and hybrid simulations and compare to the sound velocity.
- Can you explain the fluid behavior of the RG1 system (i.e. the propagation of a quasi-sound wave) by observing the motion of the particles shown in figure 4?
- ...

4 Strong perturbations (PT2)

Contrary to the experiment in section 3 we do now address the case of a velocity perturbation of the order, or larger, with respect to the sound speed $c = \sqrt{\gamma T}$. As for the simulations in section 3 the initial condition is translationally invariant in the y direction, i.e. the simulations are one dimensional.

4.1 Fluid case: simulations A1a and A1b

The two simulations do only differ by the fluid temperature. In simulation A1a the temperature is $T=1$ while in simulation A1b $T=0.01$.

Use the MHD code & simulation A1a. Open a terminal and change to the main folder of the code (e.g. where the file `makefile` is located). Start the simulation by typing `./run_CIAS/run_A1a.sh` Under successful compilation and execution, the full path to the folder where the results are stored is written to the terminal.

6. The condition $p_i \ll p_e$ stems from the fact that the ion acoustic mode is potentially damped by Landau damping on the ions or the electrons. For the wave to propagate over a distance larger than one wavelength without being damped, its phase speed must be larger than the ion thermal speed (so that the number of ions undergoing Landau resonance is small) and much smaller than the electron thermal speed (so that the phase speed of the wave falls into the region where the electron distribution function is flat). Note that in the hybrid code, electrons are treated in the fluid approximation so that no Landau damping is possible on the electron distribution function.

7. In a collisional fluid the value of the adiabatic index γ is generally well approximated by $\gamma = (l+2)/l$ where l is the number of degrees of freedom which can absorb energy. For point particles (e.g. atoms) $l=3$, corresponding to the three translational directions in space. For bi-atomic molecules (e.g. air) $l=5$ as there are also two rotational degrees of freedom. If the motion of the particles is constrained by the magnetic field and there are no collisions to redistribute energy in the direction transverse to the field, $l=1$ (i.e. $\gamma=3$) is a good approximation.

Change to the folder where the results are stored (e.g. the file [A1a_xy_all_0000.csv](#)) and start ParaView by typing the command [paraview &](#)

Once inside the ParaView window, select the tab [File → Load State](#) and select the state [A1a_comparative_view.pvsm](#) in the sub folder [PVSM_CIAS](#) of the main code folder. In the Load State Options window select the option [Choose File Names](#) and load all files generated by the simulation by right-clicking on the Group [A1a_xy_all_...](#)[csv](#) After loading the group of files the following image should appear in the ParaView “RenderView” window:

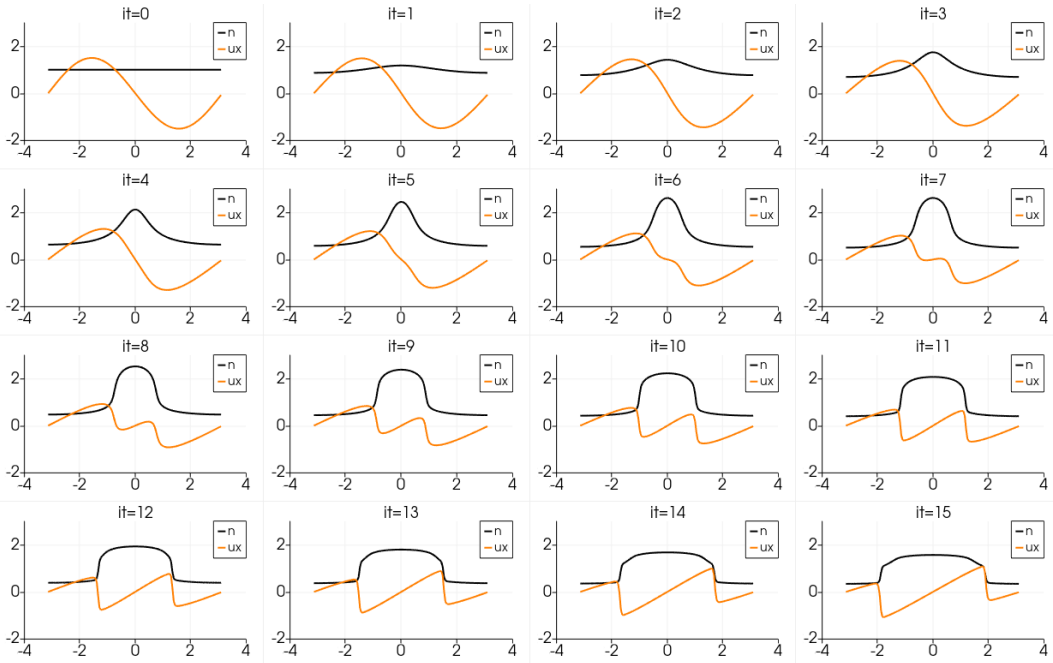


Figure 5. Time evolution of the density n and fluid velocity u_x in simulation A1a. The figure has been obtained with the state file [A1a_comparative_view.pvsm](#).

Note that here the initial velocity profile u_x is sinusoidal and not bell-shaped as in the experiment of section 3 and, more importantly, the amplitude of the initial velocity fluctuation is comparable to the sound velocity ($c = \sqrt{\gamma T} = 1.29$).

Observations:

- The initial steepening of the velocity profile \rightarrow density growing near the center reaching a maximum at $it=6$.
- The pressure gradient which builds up during the initial phase pushes the fluid away from the central region and generates two shocks (sharp density and velocity gradients) propagating in opposite directions.
- ...

Use the MHD code & simulation A1b: Open a terminal and change to the main folder of the code (e.g. where the file `makefile` is located). Start the simulation by typing `./run_CIAS/run_A1b.sh`, change to the folder where the results are stored and start ParaView with the command `paraview &`. Use the state file `A1b_comparative_view.pvsm` to produce the following figure:

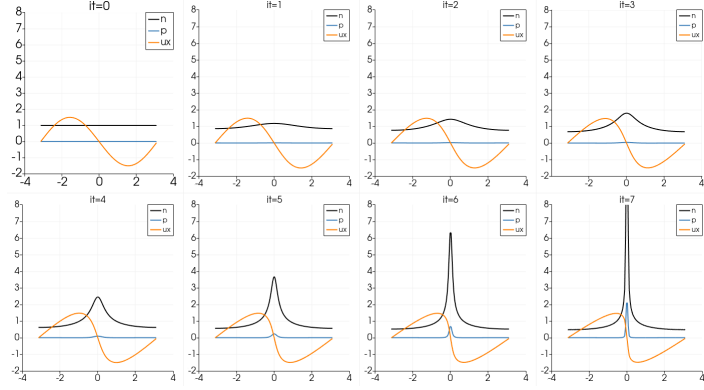


Figure 6. Time evolution of the density n and fluid velocity u_x in simulation A1b where the temperature is 100 times lower than in A1a. The figure has been obtained with the state file `A1b_comparative_view.pvsm`.

We note that in simulation A1b the pressure which builds up at the center is too small to avoid the fluid to concentrate there leading to increasingly strong gradients and, eventually, to a numerical catastrophe.

Sample questions:

- What determines the time t^* (linear time scale or steepening time scale) corresponding to the formation of the steep gradients in simulations A1a and A1b ?
- What happens in case A1b in the limiting case $T \rightarrow 0$ (assuming an infinite spatial resolution of the numerical grid)?
- ...

4.2 Hybrid case:

All simulations have the same initial sinusoidal velocity profiles as in the fluid case of the preceding section. Temperatures for protons and electrons are initialized as shown in the table (Remember, in the hybrid code, the normalized temperatures are related to β via $T = \beta/2$):

Run	RG1B4	RG1B4a	RG1B3
$\beta_e = 2T_e$	0.01	0.25	0.5
$\beta_p = 2T_p$	0.01	0.01	0.05

Cold electron case (RG1B4)

The proton dynamics in the phase space (x, u_x) for the case RG1BA is shown in the next figure. The simulation can be seen as the collisionless version of A1b. Protons are essentially free streaming with no force acting on them.

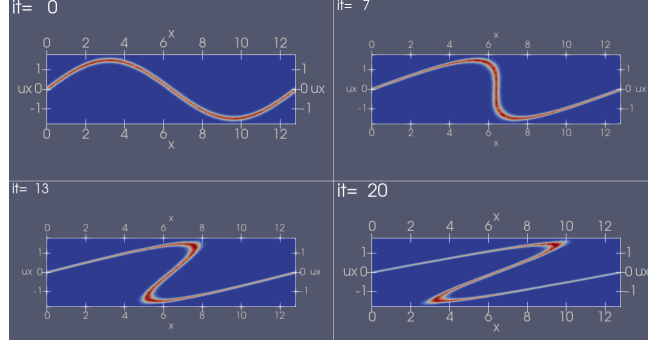


Figure 7. Evolution of the particles (protons) in the phase space (x, u_x) for the case RG1B4. Color scale indicates the particles' phase space density. The plot has been obtained using the state file [RG1B4_f_vx_x_4.pvsm](#).

During the late phase of the evolution, in some regions of space, three distinct populations of protons with distinct average velocity coexist without any notable interaction.⁸ This is illustrated in the next figure:

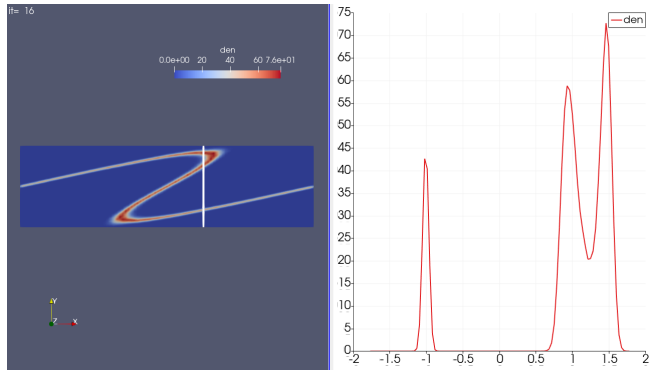


Figure 8. Simulation RG1B4 obtained using the state file [RG1B4_f_vx.pvsm](#). Is traced, in the right panel, the proton velocity distribution function $f(x, v_x)$ along the path $x = 8$ (white line in the phase space plot of the left panel).

The time evolution of the fluid quantities for RG1B4 is shown in the next figure.

⁸. In a collisional plasma there is only one population per species. Except for possible small deviations due to macroscopic gradients in the system, at any given time t and position \mathbf{x} , the velocity distribution function is fully specified by a Maxwell-Boltzmann velocity distribution function $f(\mathbf{v}) = f_{\text{MB}}(\mathbf{v}) = n(2\pi T)^{-3/2} \exp[-(\mathbf{v} - \mathbf{u})^2/2T]$, where n , T and \mathbf{u} are the local density, temperature and fluid velocity, respectively. On the other hand, if collisions are rare, there is no a priori mechanism to prevent $f(\mathbf{v})$ to depart significantly from $f_{\text{MB}}(\mathbf{v})$ for a given species in the system. In many cases it is however possible to split $f(\mathbf{v})$ in a sum of a number of simple functions $f(\mathbf{v}) = f_1(\mathbf{v}) + f_2(\mathbf{v}) + f_3(\mathbf{v}) + \dots$. One may then loosely call each $f_i(\mathbf{v})$ a population. In the right panel of Fig. 8 three distinct populations are clearly identifiable.

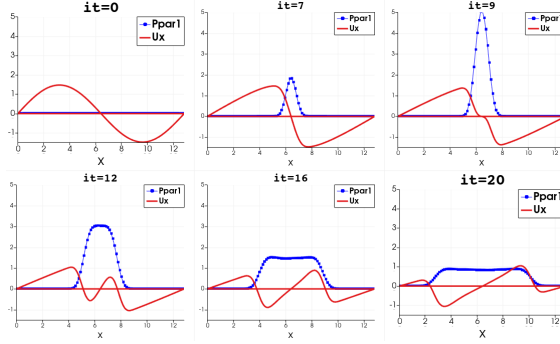


Figure 9. Simulation RG1B4, obtained using the state file [RG1B4_6.pvsm](#)

NB: Fluid quantities such as the fluid velocity u , the number density n , the pressure p and the heat flux q are defined as the moments of the distribution function f . In the general case $f = f(t, \mathbf{x}, \mathbf{v})$ is a function of time t and the 6 coordinates of the phase space (\mathbf{x}, \mathbf{v}) . In the case where the particles' motion is one-dimensional (as in the present case) one has:

$$n = \int dv f(v), \quad nu = \int dv v f(v), \quad p = \int dv (v - u)^2 f(v), \quad q = \int dv (v - u)^3 f(v)$$

The temperature is defined as $T = p/n$.

Sample questions:

You may address various questions by noting that the distribution function can be approximated at any position x by $f = \sum_i n_i \delta(v_i)$ where n_i and v_i are the density and the velocity of the various branches of the distribution function.

- How do you explain the high pressure building up in the center ?
- Can you give an estimate of the maximum temperature at the center as a function of the parameters of the initial condition ?
- Can you plot (by hand on a figure or using ParaView) the fluid velocity u in the left panel of Fig. 8 (you may help yourself by producing a figure similar to Fig. 11 and plotting u in place of E in the right panel).
- What can you tell about the heat flux q ?
- In order to approximate a collisionless system using a fluid model one has to choose a closure relation⁹. A simple possible closure which works dimensionally could be $q = Apu$ where A is a numerical constant p the pressure and u the fluid velocity. Could such a closure apply to the above case ?

9. For example, in standard MHD, the adiabatic closure is generally used. In a polytropic fluid, the adiabatic closure can be written as $(\partial/\partial t + \mathbf{u} \cdot \nabla \mathbf{u})(p/\varrho^\gamma) = 0$ where p , ϱ and \mathbf{u} are the pressure, the mass density and the fluid velocity, respectively.

● ...

Warm electron case (RG1B4a)

The main difference with respect to case RG1B4 is that the pressure of the electrons is no longer negligible. As a consequence, the gradients of the electron pressure which appear in the system induce a sufficiently strong electric field to affect the protons' trajectories as shown below:

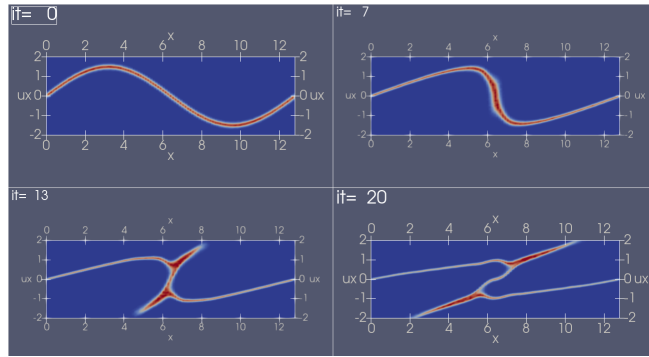


Figure 10. Evolution of the particles (protons) in the phase space (x, u_x) for the case of RG1B4a. Color scale indicates the phase space density of the particles. The plot has been obtained using the state file [RG1B4_f_vx_x_4.pvsm](#).

In particular, with respect to the case RG1B4, in RG1B4a some of the protons are accelerated to form beams of high velocity (with respect to the simulation frame). The spatial profile of the electric field can be plotted using the state file [RG1B4a_f_vx_x_Ex.pvsm](#)¹⁰ which produces the following image:

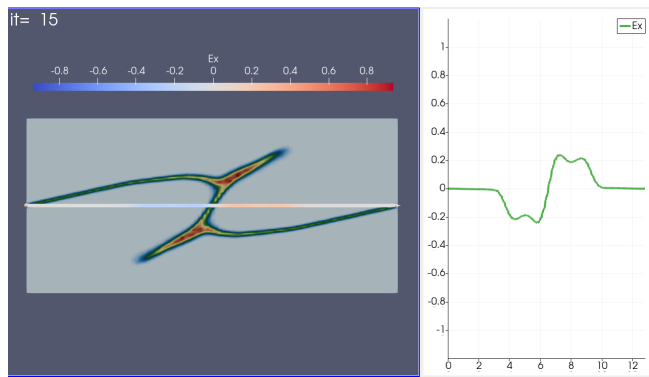


Figure 11. Simulation RG1B4a obtained using the state file [RG1B4a_f_vx_x_Ex.pvsm](#) showing the proton distribution function $f(x, v_x)$ on the left and the spatial profile of the x component of the electric field $E_x(x)$ on the right.

¹⁰. Note that when this state file requires that two groups of files being loaded: the group with the particles (files of the type [Part_5D_...](#)) and the group with the electric field (files of the type [..._E_...](#))

Cuts through the distribution function $f(x, v_x)$ can be plotted by re-using the state file [RG1B4_f_vx_x.pvsm](#) as done here for the case RG1B3:

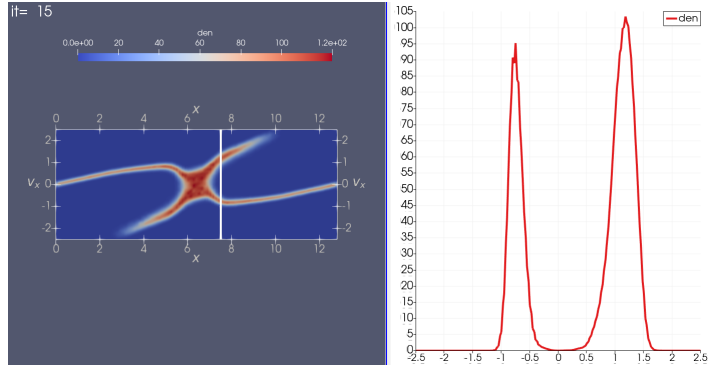


Figure 12. Simulation RG1B3 obtained using the state file [RG1B4_f_vx.pvsm](#). Is shown, in the right panel, the proton velocity distribution function $f(x, v_x)$ measured along the path in phase space at $x = 8$ (white line in the phase space plot in the left panel).

Sample questions:

- Where do the high energy protons come from ? By what are they accelerated ?
- Discuss differences between RG1B4 and investigate the differences with respect to RG1B4a
- Differences between RG1B4a and RG1B3?
- ...

5 The ion beam instability (PT3)

In the previous section (Section 4.2) we have noted that in a collisionless plasma more than one population of protons may coexist at one given place (the same may happen for electrons but obviously not in a hybrid code where electrons are treated as a fluid). In a collisional plasma such a coexistence is not possible as collisions immediately thermalize all populations into a single one.

In this section we address the question of the stability of two populations of protons streaming one respect to the other along the local magnetic field, a situation often encountered in collisionless plasmas. As we shall see, nature and strength of the instability varies with the plasma parameters (density, magnetic field strength, relative velocity, temperature, ...).

In general, an instability arises if a mode exists with phase speed such as to be able to increase its amplitude by taking the kinetic energy from the beam particles. For this to happen, phase velocity and beam velocity must be quasi-equal in which case the mode is said to resonate with the beam.

5.1 Electrostatic case (run M1)

A particular example of beam instability is the one involving the ion-acoustic mode. The ion acoustic mode is a plasma equivalent of the standard acoustic mode in a compressible gas. Its phase speed is $(\omega/k)^2 = c_s^2 = (T_e + 3T_p)/m_p$ in proton-electron plasma. The very fact that the phase speed does not depend on the magnetic field, suggest that the mode is a purely electrostatic one, not associated with fluctuations of the magnetic field. As already anticipated a beam of protons is potentially unstable if the phase speed of a plasma mode is roughly the same as the beam velocity. To be more precise, a mode can grow (and be unstable) if its phase speed falls in the velocity interval where the slope of the beam distribution function is positive as shown in the next figure for the case of the ion acoustic mode with phase speed $\omega/k = c_s$.

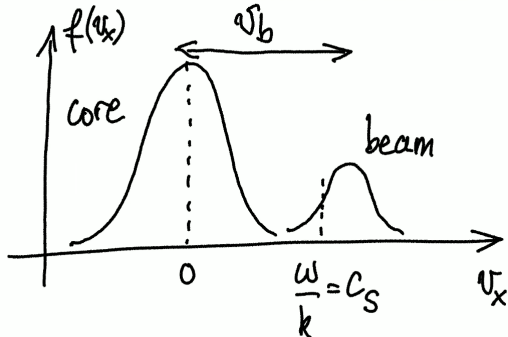


Figure 13. The ion acoustic mode can be excited by the beam if its phase speed is falls within the region where the slope of the velocity distribution function is positive $df/dv_x > 0$. If so, selected particles in the beam loose their kinetic energy to the wave.

In this example (where the magnetic field plays no role) the condition for instability is $\omega/k = c_s \approx v_b$ or, stated differently $\omega/k - v_b \approx 0$. On average, beam particles will loose kinetic energy (by moving towards the core) which is transferred to the wave.

The plasma parameters for the simulation M1 are summarized in the following table.

	v_b	$\beta_e = 2T_e$	$\beta_{core} = 2T_c$	T_b/T_c	n_b/n_c
M1	0.7	0.5	0.05	1	0.1

The density and pressure of the beam are 1/10 of the values in the core which implies that the ion acoustic propagation speed is essentially given by the core plasma, i.e. $c_s = \sqrt{T_e + 3T_c} \approx 0.57$.

Note that in the simulation (in order to improve statistics for the beam particles) the same number of particles has been used for core and beam. Given that $n_b/n_c = 0.1$, the statistical weight of a core particle is 10 times that of a beam particle.

As for the other simulations based on the hybrid code the simulation must be started from within the `input` folder with the command `./run ./run_CIAS/M1.in`. Using the state file `M1_vx_x_2_pop.pvsm` to load the protons from the beam and the core into ParaView it is possible to visualize the evolution of the instability in phase space as shown in the next figure¹¹.

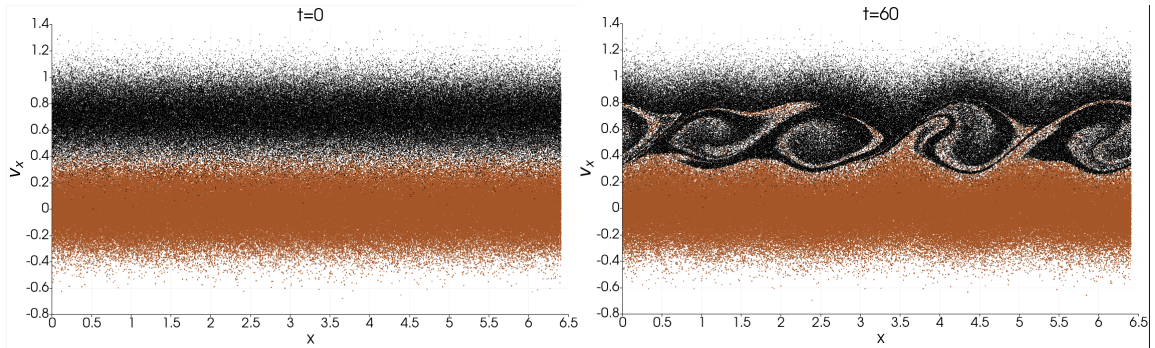


Figure 14. Simulation M1 showing the core and beam protons in phase space. Shown are the initial state and the evolved state when the ion beam instability has entered the non-linear phase of the instability. Figure obtained with the state file `M1_vx_x_2_pop.pvsm`

The electric field can be over-plotted on the phase space plot by using the state file `M1_vx_x_E.pvsm`:

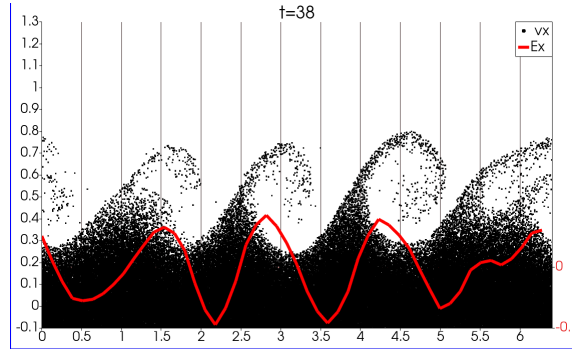


Figure 15. Core particles and electric field profile in simulation M1. The state file `M1_vx_x_E.pvsm` has been used here. Obviously, the same state file can be used to plot the beam particles.

As shown in the next figure, the local (i.e. in a limited spatial range) core and beam velocity distribution functions can be plotted using `M1_vx_x_hist.pvsm`

¹¹. Note that you will have to provide both populations to the state file: `Part_5d_ascii1M1..` and `Part_5d_ascii2M1..`

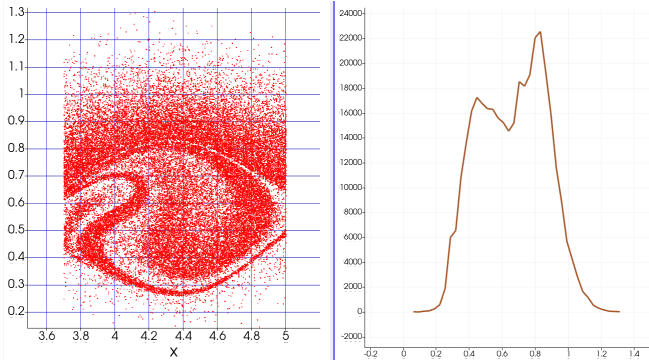


Figure 16. Case M1: velocity distribution function $f(v_x)$ for the beam protons in the range $x \in [3.7, 5]$. State file used for the plot: [M1_vx_x_hist.pvsm](#)

Sample questions:

- Estimate the linear growth rate Γ of the instability. Give the wavelength λ of the dominant mode.
- Try to observe the deformation of the proton distribution function during the linear phase of the instability (see Section 5.1.1)
- What happens during the non-linear phase of the instability (trapping of particles by the electric field) ?
- ...

5.1.1 Physical interpretation of the electrostatic ion-beam instability

Let us assume that, as a result of the statistical fluctuations an ion acoustic mode with a wave vector $k = 2\pi/\lambda$ appears in the core-beam system. The mode being a purely electrostatic one, it can be shown that the electrostatic field fluctuation $\delta\phi$ and the density fluctuation δn must vary spatially in phase¹². Let us then ask, if the wave which propagates at a speed $c_s = \omega/k$ as shown in Figure 13 is compatible with an exponential growth in time at the rate Γ . To answer the question we verify whether or not some of the natural density fluctuations δn which are naturally present in the system grow exponentially in time out of the initial “noise”¹³. If yes the mode is unstable.

It is important to realize that given the (a priori unknown) grow rate Γ and the wave vector k , two categories of particles exist. The resonant particles, with $|v - c_s| < \Gamma/k$, and the circulating particles¹⁴. The circulating particles are moving sufficiently fast with respect to the wave so that during the characteristic growth time of the instability Γ^{-1} they travel a distance larger than λ . On average the velocity of

¹². We remember that in the electrostatic limit (where the magnetic field plays no role) the electric field depends on the gradient of the electron pressure via $E \propto -\nabla p_e$. Assuming a constant temperature, one has $E = -\partial\phi/\partial x \propto -\partial\delta n/\partial x$ meaning that $\delta\phi$ and δn must vary in phase.

¹³. Density fluctuations are due to the fact that the number of particles per cell is finite. The relative amplitude of the density fluctuations at cell level $\delta n/n$ is of the order $\sqrt{N_c}/N_c$ where N_c is the number of particles per cell.

¹⁴. Obviously, the resonant region can extend over the whole portion of the distribution function with $\partial f/\partial v > 0$.

these particles is unchanged as they have traveled through a spatially oscillating electrostatic potential with no net gain of energy. On the other hand, during the same time interval Γ^{-1} , the resonant particles travel over a distance smaller than λ and either gain or loose kinetic energy depending on whether they are located in a trough or a bump of the electrostatic potential $\phi(x)$.

The evolution of the beam velocity distribution function in electrostatic field of a growing ion acoustic wave with phase speed located in the region of positive $\partial f / \partial v > 0$ is shown in figure 17. In a deepening potential trough, resonant particles constantly increase their velocity implying a shifting of the distribution towards higher velocities (red curve). On the other hand, in a growing potential bump, resonant particles constantly decelerate and the distribution shifts towards lower velocities (blue curve). As a consequence, the density increase in potential bumps and decreases in potential troughs further accentuating the initial density fluctuation: the configuration is unstable. If the phase velocity of the wave is located in the region with $\partial f / \partial v < 0$, the density evolution in troughs and bumps would be such as to reduce (damp) the initial fluctuation: the configuration is stable.

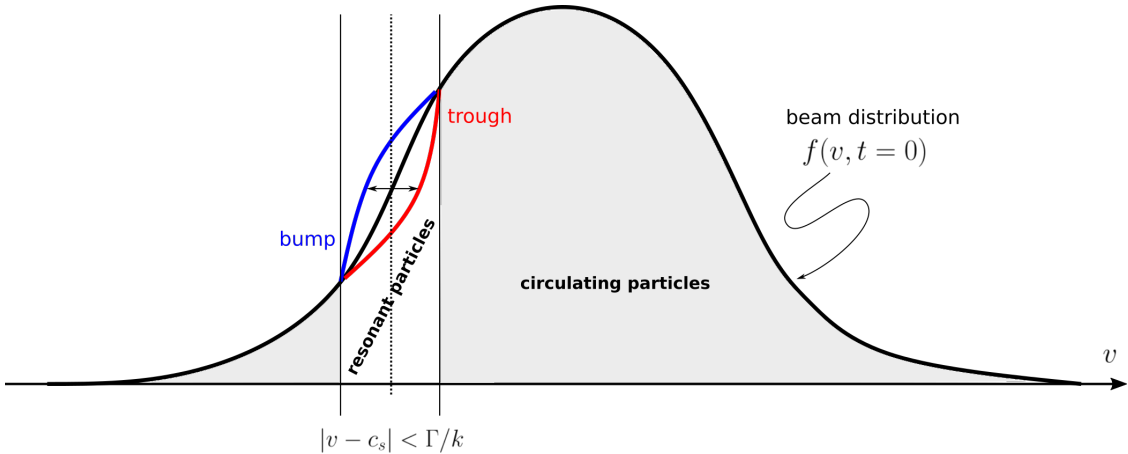


Figure 17. Deformation of the ion beam velocity distribution function in the field of a growing ion acoustic wave with its phase velocity located in the region of positive slope of the distribution function f . Note that the evolution from the black to the red/blue profiles is only noticeable over time scales $>\Gamma^{-1}$. The distribution of the resonant particles is a spatial average in troughs or bumps, the distribution of the circulating particles is averaged over a distance $l\lambda$ where l is an integer number.

5.2 Electromagnetic case (run M2)

In this example, as in M1, we consider the case of a beam of protons streaming along a magnetic field line $\mathbf{B}_0 = B_0 \hat{x}$ where \hat{x} is the unit vector in the x direction. As in the case M1, an instability arises if there is a plasma mode which can resonate with the beam. Here, however, we do now consider a combination of plasma and beam parameters such as to drive unstable either the Alfvén Ion Cyclotron (AIC) mode or the magnetosonic whistler (MW) mode.

	v_b	$\beta_e = 2T_e$	$\beta_{\text{core}} = 2T_c$	T_b/T_c	n_b/n_c
M2	$2.5v_A$	0.0005	0.1	1	0.2

In the next figure the dispersion relations for the AIC and the MW modes are plotted in the cold plasma limit, i.e. for $\beta \ll 1$ which is fine here (see above Table).

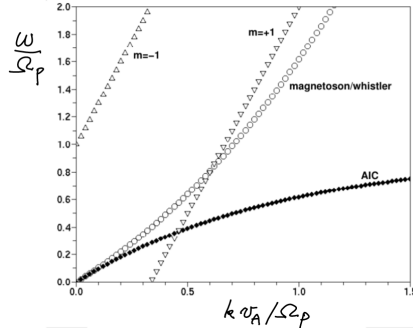


Figure 18. Dispersion relation for the AIC mode and the magnetosonic/whistler mode. Added, as examples, are the resonance curves computed from 8 based on a beam velocity $v_b = 3v_A$.

For small values of k (long wavelength) both the AIC dispersion and the MW dispersion merge with the Alfvén mode $\omega/k = \pm v_A$. As k increases the phase speed ω/k decreases for the AIC while it increases for the MW (the modes become dispersive). The characteristic spatial and temporal scales at which the phase velocity of the two modes separate are of the order v_A/Ω_p and Ω_p^{-1} , respectively (where $\Omega_p = eB_0/m_p$ is the proton angular frequency).¹⁵

Again, as for the M1 case instability of the beam is only possible if there is a plasma mode such that the resonance condition can be satisfied

$$\omega + m\Omega_p \approx kv_b \quad (8)$$

where m is an integer number ($m = 0$ in the electrostatic case M1). The resonance curves for $m = \pm 1$ are plotted in Figure 18 for a beam with $v_b = 3v_A$ showing that the resonance curve $m = +1$ crosses the AIC and MW for $kv_A/\Omega_p \approx 0.5$ ¹⁶

The instability of the beam in M2 can be explored using the state file `M2_f_vx_x_B.pvsm`. The magnetic nature of the instability is clearly visible in the figure (growing oscillations of the magnetic field):

15. In an electro-proton plasma $c/\omega_p = v_A/\Omega_p$ is called the proton inertial length with $\omega_p = \sqrt{m_p/\epsilon_0 e^2 n}$ being the proton plasma angular frequency. Hybrid codes are particularly adapted to simulate a plasma at these scales. As a consequence, grid points in hybrid simulations are separated by distances of order $\lesssim c/\omega_p$.

16. The crossing of the resonance curve with the dispersion relation of a plasma mode is not a sufficient condition. For the resonance to be effective, in the frame of the resonating particles, particles and the wave must rotate together.

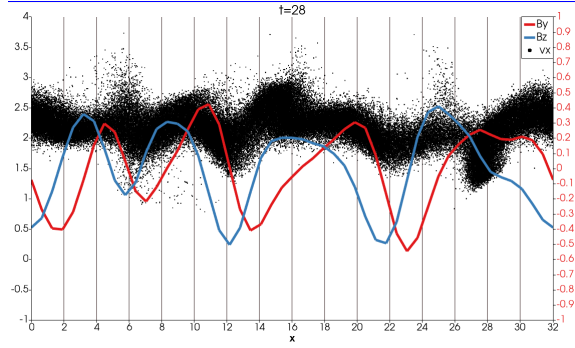


Figure 19. Simulation M2. Beam particles and transverse magnetic field components.
State file: [M2_f_vx_x_B.pvsm](#).

The two transverse components of the magnetic field B_y and B_z and the associated hodogram can be plotted using the state file [M2_B_hodo.pvsm](#):

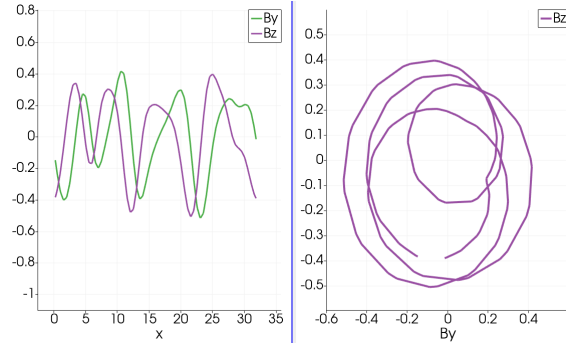


Figure 20. Simulation M2. Transverse components of the magnetic field lines as a function of x (left panel) and hodogram showing the rotation of the vector (B_y, B_z) when moving along the x axis. Note the circular polarization of the mode.

In the next figure are plotted all protons (beam and core) from the simulation M2 in the phase space (v_x, v_z) . Interestingly, the beam particles tend to describe a circular arc centered on the phase velocity of the wave.

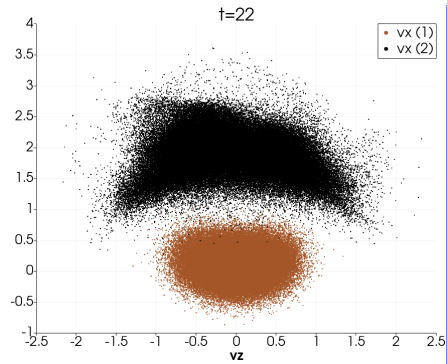


Figure 21. Phase space (v_x, v_z) with all beam and core protons from simulation M2.
Figure has been obtained using the state files [M2_vx_vz_both_pop.pvsm](#).

Sample questions:

- Measure the propagation speed of the wave and the growth rate of the instability.
- Is the unstable wave an AIC or a MW wave ?
- What is the polarization of the wave in the plasma frame (essentially the simulation frame), i.e. does the magnetic field rotate clockwise or anticlockwise when looking in the direction of the propagating wave ?¹⁷
- What is the phase speed of the unstable mode required to satisfy the resonance condition 8 with $m = +1$? Why is the resonance condition different with respect to the electrostatic case M1 ?
- Verify that in the frame of the resonating particle the wave rotates in phase with the protons.
- In figure 21 the beam particles describe an arc. Can you comment on this by considering that in the wave frame the electric field is essentially zero¹⁸
- ...

5.2.1 Derivation and general properties of the MW and AIC waves

The main characteristics of both the MW and the AIC modes can be obtained relatively easily in the cold plasma limit. At large scales, i.e. for $k \rightarrow 0$, both modes propagate at the Alfvén speed. However, at scales of the order of the proton inertial scale v_A/Ω_p and the proton gyration period Ω_p^{-1} , a drift of the protons with respect to the electrons becomes possible in the direction perpendicular to the magnetic field lines. At these scales both modes become dispersive¹⁹. The relative drift of the protons with respect to the electrons in the direction perpendicular to \mathbf{B} is called the Hall effect. In order to account for the Hall effect, an additional, current dependent term, has to be added in Ohm's law:

$$\mathbf{E} = -\mathbf{u} \times \mathbf{B} + \frac{\mathbf{j} \times \mathbf{B}}{en}, \text{ where } \mathbf{j} = en(\mathbf{u} - \mathbf{u}_e) \quad (9)$$

where \mathbf{u} is the mean velocity of the plasma (but also of the protons as $m_e = 0$) and \mathbf{u}_e the mean velocity of the electrons which can only move along the magnetic field lines. It should also be noted that the ideal term $-\mathbf{u} \times \mathbf{B}$ is frame dependent while the Hall term is not.

17. The polarization is often called left-handed (anticlockwise) and right-handed (clockwise).

18. A plasma carrying a magnetic field \mathbf{B} at a speed \mathbf{u}_0 generates an electric field $\mathbf{E} = -\mathbf{u}_0 \times \mathbf{B}$ in the rest frame and corresponds to the first order (in u/c) Lorentz transformation of the electric field from the plasma frame to the rest frame. Note that the magnetic field is frame invariant to first order in u/c .

19. Dispersive in the sense that the phase speed ω/k is not a constant but dependent on k .

Assuming a plasma equilibrium with a magnetic field pointing in the x direction $\mathbf{B}_0 = B_0 \hat{\mathbf{x}}$ and a proton density $\rho_0 = m_p n_0$ we write the fluid equations for the fluctuating quantities (labeled δ):

$$\delta \mathbf{E} = -\delta \mathbf{u} \times \mathbf{B}_0 + \frac{\delta \mathbf{j} \times \mathbf{B}_0}{en_0} \quad (\text{Ohm's law}) \quad (10)$$

$$\rho_0 \frac{\partial}{\partial t} \delta \mathbf{u} = \delta \mathbf{j} \times \mathbf{B}_0 \quad (\text{equation of motion}) \quad (11)$$

$$\frac{\partial}{\partial t} \delta \mathbf{B} = -\nabla \times \delta \mathbf{E} \quad (\text{Faraday}) \quad (12)$$

$$\delta \mathbf{j} = \nabla \times \delta \mathbf{B} \quad (\text{Ampère}) \quad (13)$$

We assume 1D fluctuations $\propto \exp[i(kx - \omega t)]$ ²⁰ and incompressible fluctuations so that $\delta u_x = \delta B_x = 0$ ²¹. After some algebra work (noting that $\partial/\partial t = -i\omega$ and $\nabla \times = ik\hat{\mathbf{x}} \times$), we obtain the dispersion relation for the MW (“+” sign) and the AIC (“−” sign) propagating modes:

$$\tilde{\omega} = \frac{1}{2} \tilde{k} \left(\tilde{k} \pm \sqrt{4 + \tilde{k}^2} \right), \text{ where } \tilde{\omega} \equiv \frac{\omega}{\Omega_p} \text{ and } \tilde{k} \equiv \frac{k v_A}{\Omega_p} \quad (14)$$

The $+/-$ sign corresponds to the MW and the AIC mode, respectively. The equation shows that for $\tilde{k} \rightarrow 0$ one has $\omega/k = \pm v_A$, i.e. both modes propagate at the Alfvén speed in the long wavelength limit.

The two solutions are plotted in the following figure

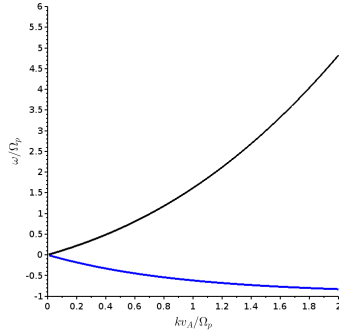


Figure 22. Dispersion relation $\omega(k)$ for the MW mode (upper black curve) and the AIC mode (blue curve) in the cold plasma limit. The frequency of the AIC mode is negative as it propagates in the direction opposite with respect to the MW mode.

An interesting conclusion can be deduced from the Faraday equation which implies that for the two modes we have

$$\frac{\omega}{k} \frac{\delta \mathbf{B}}{B_0} = \mathbf{B}_0 \times \delta \mathbf{E} \quad (15)$$

²⁰ We also assume $k > 0$ while ω may be complex (for example for a damped mode $\text{Im}(\omega) < 0$).

²¹ Incompressible means $\nabla \cdot \delta \mathbf{u} = 0$. On the other hand, Maxwell’s equations imply $\nabla \cdot \delta \mathbf{B} = 0$.

and therefore (since ω is real) that electric and magnetic field fluctuate perpendicularly to each other and that $|\delta\mathbf{B}|$ and $|\delta\mathbf{E}|$ are constant which implies circular polarization, e.g. $\delta B_y = \pm i \delta B_z$. In this context, we note that wave polarization is often defined as $P \equiv \delta B_y / i \delta B_z = \pm 1$, the sign indicating the sense of rotation of the magnetic field in the plasma frame. With this definition, it turns out that the MW mode corresponds to the case $P = +1$ (right-handed) and the AIC to $P = -1$ (left-handed)²². The other interesting consequence of the above equation is that the electric field fluctuation vanishes in the wave frame (can you show?).

From Ampère's equation it also follows that the current fluctuates parallel or anti-parallel to $\delta\mathbf{B}$ depending on the polarization, i.e.

$$\delta\mathbf{j} = -Pk \delta\mathbf{B} \quad (16)$$

From Ohm's law and Faraday's equation it follows that the velocity fluctuation is

$$\delta\mathbf{u} = -\left(P \frac{k v_A^2}{\Omega_p} + \frac{\omega}{k}\right) \frac{\delta\mathbf{B}}{B_0} \quad (17)$$

indicating that the fluid oscillates in opposition to the magnetic field for the MW mode (for which $P, \omega > 0$) whereas $\delta\mathbf{u}$ and $\delta\mathbf{B}$ oscillate in phase for the AIC mode (for which $P, \omega < 0$).

It should be noted that in the above calculation ω is real, a consequence of the cold plasma assumption. In a mild or warm plasma, when approaching $\tilde{k} \sim 1$, ω develops a negative imaginary part for both modes corresponding to wave damping. In particular, at $\tilde{k} \gtrsim 0.5$, because of a $m = -1$ resonance, the AIC mode is generally heavily damped.

5.2.2 Triggering the ion-beam instability

Under favorable circumstances, a beam of ions drifting along the magnetic field with respect to a population of resting ions can amplify one of the two electromagnetic modes discussed in the Section 5.2.1. As already mentioned earlier a wave may grow in time through the conversion of the kinetic energy contained in the distribution function to wave energy. A possible favorable circumstance is resonance involving a mode of the plasma (for example the MW or the AIC) and the protons of the beam as illustrated in Figure 18. However, the fact that a plasma mode with given ω and k satisfies to the resonance condition 8 may not be a sufficient condition for the mode to be able to extract the energy from the beam particles. For example, in Figure 18 the $m = +1$ resonance condition crosses the dispersion curve of both the MW and the AIC mode but, as we have seen in the simulation, only one of the two modes has been destabilized by the beam. The fundamental reason is polarization. As discussed in Section 5.2.1, in the plasma frame (which is essentially the frame of the core population if the beam density is small), the magnetic field vector or

²² NB: the rotation of a proton in a magnetic field is left-handed.

the electric field vector are right-handed for the MW mode and left-handed for the AIC mode meaning that for an observer at a fixed position the sense of rotation of the electric field is opposite for the two modes. Now, an efficient energy exchange between the wave and the beam particles can only take place if the resonant particles experience a net acceleration (or deceleration) in the rotating electric field. For example a proton traveling with the wave conserves its energy as for both the MW and the AIC the electric field vanishes in the wave frame (see Section 5.2.1). This is the reason for the resonance condition $\omega/k \approx v_b$ not to be the pertinent one as for the electrostatic case discussed in Section 5.1. Remembering that the electric field of the MW and the AIC modes is perpendicular to \mathbf{B}_0 and that protons make a left-handed rotation about \mathbf{B}_0 one deduces that for the beam particles to constructively resonate with the wave they must see the wave electric field to make a left-handed rotation about \mathbf{B}_0 in their own frame, i.e. in the beam frame.

Let us consider the MW wave which is right-handed in the plasma rest frame. A proton traveling in the direction of propagation of the wave (i.e. in the direction of \mathbf{k} or \mathbf{B}_0) at a speed lower than the wave speed ω/k it will see the electric field of the wave rotate against its proper cyclotron rotation. A proton traveling at $v > \omega/k$ will see the wave field make a left-handed rotation. A proton traveling at $v = (\omega + \Omega_p)/k$ sees the wave field rotate at the angular velocity Ω_p and becomes accelerated perpendicularly to \mathbf{B}_0 (and $\delta\mathbf{B}$) at a rate $dv_\perp/dt = e\delta E/m$ where $\delta E = \Omega_p \delta B/k$ is the wave field from Section 5.2.1. The coherent acceleration of the beam protons in the direction perpendicular to $\delta\mathbf{B}$ is illustrated in Figure 23 for the case of a core-beam plasma with a core temperature 4 times larger than the beam temperature.

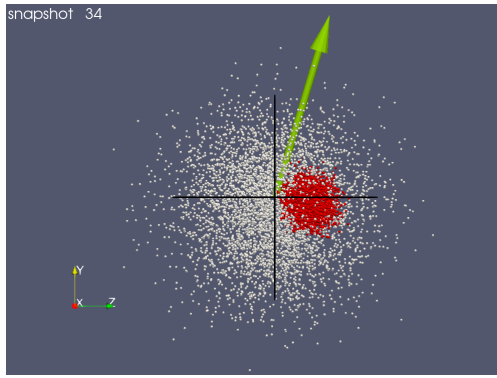


Figure 23. 1D electromagnetic proton beam instability, linear phase. Shown are the beam protons (red) and core protons (white) from a small interval along the x axis in the velocity space (v_y, v_z). Also shown is the orientation of $\delta\mathbf{B}$. Note the velocity displacement of the beam protons (initially centered in $(v_y, v_z) = (0, 0)$) in the direction perpendicular to $\delta\mathbf{B}$. Figure obtained using the state file M2_B_vy_vz_local.pvsm.

It must be noted that the core particles do experience an electric field of amplitude $\delta B \omega/k$ (in the direction opposite of that of the beam particles) but the field is a fluctuating one which averages to zero so that the core protons oscillate in velocity with no net gain of energy. The growth of v_\perp for the beam protons averaged over several wavelength is shown in Figure 24.

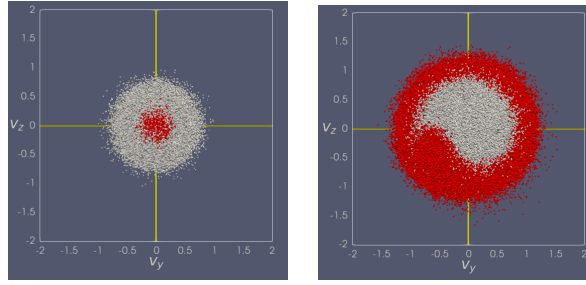


Figure 24. 1D electromagnetic proton beam instability. Protons in the (v_y, v_z) plane at $t=0$ (left) and during the linear growth of the instability (right). Shown are all beam protons (red) and core protons (white) in the system, covering a distance of several wavelength. Note the general growth of the protons transverse velocity $v_\perp = \sqrt{v_y^2 + v_z^2}$.

The figure allows for a rough insight into the physical mechanism of the instability. First: beam protons are coherently accelerated by the wave electric field in the direction perpendicular to $\delta\mathbf{B}$. At the same time the core protons are accelerated in the opposite direction. Second: due to curvature of the field lines, part of this increase in transverse velocity becomes field aligned (as shown in see Figure 25) so as to increase δu and, consequently, the wave amplitude.

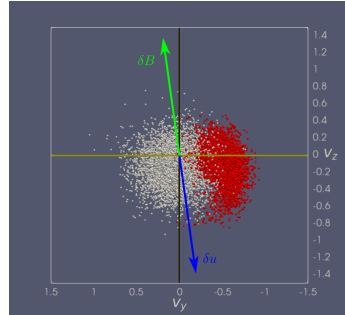


Figure 25. 1D electromagnetic proton beam instability. Protons in the (v_y, v_z) plane at $t=0$ (left) and during the linear growth of the instability (right). Shown are the beam protons (red) and core protons (white) at a given position along the x axis. Note how the protons in the beam are accelerated in the y direction and how part of this newly acquired velocity is converted into v_z velocity (in the same direction as the velocity fluctuation δu , thus contributing in increasing the fluctuation associated with the wave).

6 Mixing plasmas (PT4)

In this section we will try to mix two fluids. We will see that this is not as easy as it sounds, even in a collisionless plasmas. The initial set-up for both the MHD and

the hybrid simulations is summarized in the next figure:

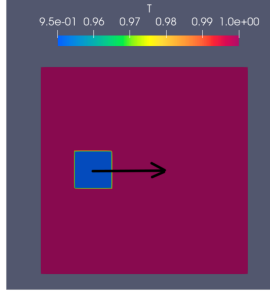


Figure 26. Initial condition for all simulations in this section. A portion of plasma (inside the square) is set in motion with respect to the outside plasma which is at rest in the simulation frame.

As shown in the figure at start (at $t=0$) only the fluid inside the square has a non zero velocity.

6.1 Fluid case (run TP2)

In this section we use the MHD code so move back to the [input](#) folder of the MHD code. You can then start the simulation as for the other MHD simulations by typing [./run_CIAS/run_TP2.sh](#). The simulation parameters are summarized in the following table:

	v_{square}	T	γ	B
TP2	0.6	1	1	0

You may notice that we have selected $\gamma=1$ for this simulation. The behavior of a plasma with adiabatic index $\gamma=1$ may be strange as, for example, shocks propagate through the plasma without heating it ²³. The advantage of setting $\gamma=1$ is that the temperature is transported passively by the fluid²⁴ which allows us to trace the fluid of the square by marking it with a slightly different temperature with respect to the surrounding plasma. This is the reason for the plasma inside the square in figure 26 having been set to be slightly cooler than the surrounding plasma (the plasma inside the square is also denser than the surrounding plasma in order to equilibrate the pressure).

²³. The case $\gamma=1$ can be interpreted as the limit of a fluid with an infinite number of internal degrees of freedom. Since in thermodynamic equilibrium energy is equally distributed among all available degrees of freedom, in order to rise the fluid temperature an infinite amount of energy must be injected.

²⁴. The MHD code is based on the adiabatic closure $(\partial/\partial t + u \cdot \nabla)(p/\varrho^\gamma)=0$, so that if $\gamma=1$, from the equation of state $T/m=p/\varrho$ (ideal gas), it follows $(\partial/\partial t + u \cdot \nabla)T=0$. Of course, this is correct only as long as non ideal effects (such as thermal conduction or numerical diffusion) are small.

The first phase of the evolution of the system is shown in the next figure

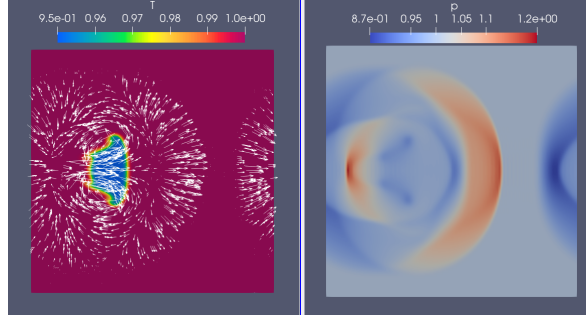


Figure 27. Initial evolution of the system with the temperature on the left (showing the displacement of the plasma which has been given an velocity at $t=0$) and the pressure on the right. Arrows in the left panel indicate the velocity field. Figure obtained using the state file [TP2_vectors.pvsm](#).

It is important to note that in the initial phase there are essentially two structures moving at very different velocities: the slow moving plasma which has been set in motion at $t=0$ (a displacement of the fluid initially in the square to the right) and a fast moving, roughly circularly shaped compressional wave (a sound wave). The displacements are best observed and analyzed in the following type of figure:

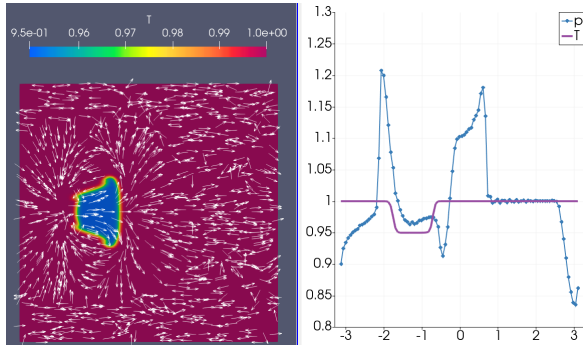


Figure 28. On the right panel: profiles of T and p along a horizontal line through the center of the simulation domain. Figure obtained using the state file [TP2_plot_over_line.pvsm](#)

One may note the slowly moving double vortex structure associated with the displacement of the initially square-shaped “cold” plasma. The fluid motion associated with the double vortex is an incompressible flow (an incompressible flow is characterized by $\nabla \cdot \mathbf{u} = 0$) while the fluid motions associated with sound waves is a compressible flow with $\nabla \cdot \mathbf{u} \neq 0$. Now, the Helmholtz theorem states that a vector field \mathbf{u} can always be decomposed in an incompressible (solenoidal) component \mathbf{u}_s and a compressible component \mathbf{u}_c , i.e. $\mathbf{u} = \mathbf{u}_s + \mathbf{u}_c$. Such a decomposition is a valuable tool to filter out the compressible component of the flow. In the next figure we plot the streamlines of the solenoidal (incompressible) part of the flow for the TP2 simulation

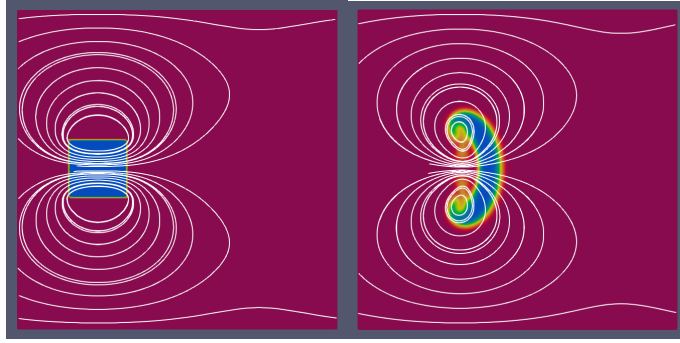


Figure 29. Simulation TP2. Streamlines of the solenoidal (incompressible) component of the fluid velocity \mathbf{u}_s at $t = 0$ (left) and at a later time. Note that the sound waves (associated with compressible fluid motions) are absolutely invisible. Figure obtained using the state file [TP2_velocity_stream_lines.pvsm](#)

Sample questions:

- Measure the phase speed of the incompressible (vortices) and compressible structures (sound waves).
- You may want to superpose the vectors of the effective fluid velocity \mathbf{u} on the streamlines of the incompressible flow \mathbf{u}_s in figure 29. What do you learn?
- Is there a relation between the initial velocity of the plasma (the plasmas inside the square at $t = 0$) and the phase speed of the vortices and the phase speed of the sound waves ?
- Is there a fluid displacement associated with the compressible waves ? Same question for the incompressible waves (vortices) ?
- Is it easy to move a fluid parcel inside a resting fluid ? Where does the injected energy goes ? Mainly into the vortices or into the sound waves ?
- ...

6.2 Hybrid case

We have seen in the previous section that mixing plasma is not that easy and that most of the initially injected kinetic energy is lost to compressible waves which carry the energy away from the injection region (the square in figure 26). In this section we use the hybrid code to simulate the same problem for 4 different combinations of plasma parameters as listed in the following table:

	v_{square}	(dx, dy)	n_{square}	$\beta_e = 2T_e$	$\beta_p = 2T$	ψ	ϕ
A3e1	0.5 v_A	0.5,0.5	1	0.5	0.25	90°	?
A3f1	0.5 v_A	0.5,0.5	1	0.05	0.25	90°	?
A3d1	0.5 v_A	0.25,0.25	1	0.5	0.25	0°	0°
A3da1	0.5 v_A	0.25,0.25	1	0.05	0.25	0°	0°

In the above table ψ is the angle of the magnetic field \mathbf{B} with respect to the (x,y) plane and ϕ the angle of \mathbf{B} with respect to the x axis. Also note that the size of the simulation cells (dx, dy) is smaller in A3d1 and A3da1.

Simulations with \mathbf{B} out of the simulation plane

To run the simulation A3e1, as for all hybrid simulations, go to the sub-folder [input](#) and type `./run ./run_CIAS/A3e1.in`. The result

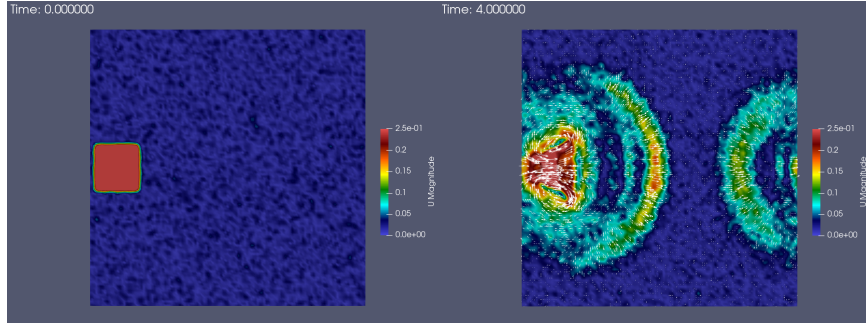


Figure 30. Simulation A3e1. Contours of the absolute value of the fluid velocity at the beginning of the simulation at $t = 0$ and at $t = 4$. Arrows indicate fluid velocity direction and magnitude. Figure produced with the state file [A3e1_2D_arrows.pvsm](#)

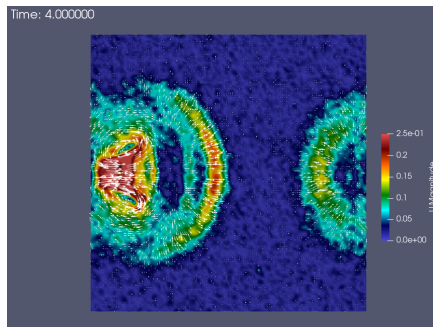


Figure 31. Simulation A3f1. Contours of the absolute value of the fluid velocity at $t = 4$. To be compared with the case A3e1. Figure produced with the state file [A3e1_2D_arrows.pvsm](#)

Simulations with \mathbf{B} in the simulation plane

In the case with the magnetic field in the simulation plane the picture changes dramatically as shown for the simulation A3da1:

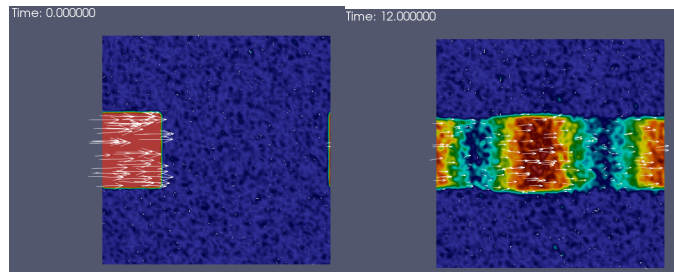


Figure 32. Simulation A3da1. Contours of the absolute value of the fluid velocity at the beginning of the simulation and at a later time. Arrows indicate fluid velocity direction and magnitude. Figure produced with the state file [A3e1_2D_arrows.pvsm](#)

The figure shows that no vortices form in this case. No compressible waves are seen propagating in the y direction (why?). On the other hand, along the x axis the behavior is qualitatively similar to that observed in the RG1 hybrid simulation of section 3.2 , showing the characteristic relation between density fluctuations and velocity fluctuations depending on the propagation direction of the wave:

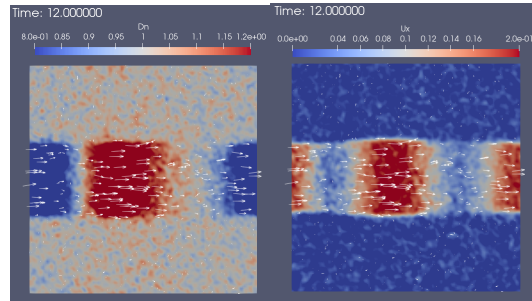


Figure 33. Simulation A3da1 at the end of the run. Density fluctuation (left) and fluctuation of u_x (right). Figure produced with the state file [A3e1_2D_arrows.pvsm](#)

Sample questions:

- Comment the notion of “plasma displacement” in a collisionless plasma.
- Are there significant differences between the fluid case of section 6.1 and the two simulations with $\psi = 90^\circ$?
- As for the fluid case you may measure the phase speed of the compressible waves. Differences between A3e1 and A3f1?
- Why are there no vortices in simulations A3d1 and A3da1
- You may want to modify the parameters of the plasma square bubble in the *.in files (for example by changing its density or its speed)
- ...